Supplementary material

The use of conductive polymers as substrate for paper spray ionization mass spectrometry

Marcella M. C. Borges,[a,#] Heloá Santos,[b,#] Géssica A. Vasconcelos,[c] Tienne A. Nascimento,[a] Flávia V. A. Dutra,[a] Bruna C. Pires,[a] João Francisco Allochio Filho,[b,e] Gloria M. F. V. Aquije,[d] Warley S. Borges,[b] Valdemar Lacerda Jr.,[b] Boniek G. Vaz,[c] Luis E. Arroyo-Mora,[f] Wanderson Romão,[b,d,*] and Keyller B. Borges[a,*]

[a] Departamento de Ciências Naturais, Universidade Federal de São João del-Rei (UFSJ), Campus Dom Bosco, Praça Dom Helvécio 74, Fábricas, 36301-160, São João del-Rei, Minas Gerais, Brazil.

[b] Departamento de Química, Universidade Federal do Espírito Santo (UFES), Av. Fernando Ferrari, 514, Goiabeiras, 29075-910 Vitória, Espírito Santo, Brazil.

[c] Instituto de Química, Universidade Federal de Goiás, Av. Esperança, Chácaras de Recreio Samambaia, 74001-970, Goiânia, Goiás, Brazil.

[d] Instituto Federal de Educação, Ciência e Tecnologia do Espírito Santo (IFES), Av. Ministro Salgado Filho, Soteco, 29106-010, Vila Velha, Espírito Santo, Brazil.

[e] Instituto Federal de Educação, Ciência e Tecnologia do Espírito Santo (IFES), Rodovia BR-101 Norte, Km 58, Litorâneo, 29932-540, São Mateus, Espírito Santo, Brazil.

[f] Department of Forensic and Investigative Science, West Virginia University, 302 Oglebay Hall Morgantown WV 26506, USA.

Correspondence:

* Prof. Keyller Bastos Borges, PhD, Departamento de Ciências Naturais, Universidade Federal de São João del-Rei, Campus Dom Bosco, Praça Dom Helvécio 74, Fábricas, 36301-160, São João del-Rei, Minas Gerais, Brazil, e-mail: keyller@ufsj.edu.br, Tel.: +55 32 3379 – 5361

* Prof. Wanderson Romão, PhD, Instituto Federal de Educação, Ciência e Tecnologia do Espírito Santo, 29106-010, Vila Velha, ES, Brazil, e-mail: wandersonromao@gmail.com, Tel.: +55 27 3149-0700

Experimental Section

Standards

The Brazilian Federal Police supplied cocaine standard (purity > 99.0%, Porto Alegre, RS, Brazil). Caffeine, phenacetin, lidocaine (99.0%, 98.0%, 98.0%, respectively, Sigma Aldrich®, São Paulo, SP, Brazil), cannabidiol (CBD), cannabinol (CBN), tetrahydrocannabinol (Δ^9-THC), abamectin (Pestanal®, analytical standard), eprinomectin (Pestanal®, analytical standard), doramectin (Vetranal®, analytical standard), moxidectin (Vetranal®, analytical standard), ivermectin (B1a, 98.97% Pharmaceutical Secondary Standard, Certified Reference Material) and estradiol valerate (European Pharmacopoeia Reference Standard) were acquired from Sigma-Aldrich® (Steinheim, Germany). Midazolam was purchased from Cristália Produtos Químicos Farmacêuticos Ltda (São Paulo, SP, Brazil), procaine from Chongqing Chuandong Chemical (Group) Co. Ltd., (Chongqing, China) and tramadol from Argon Drugs® (Maharashtra, India). Bupropion, erythrohydrobupropion, 4-hydroxybuproion, and threohydrobupropion were donated by GlaxoSmithKline® (Brentford, UK). Progesterone, medroxyprogesterone, meloxicam and meloxicam related compound C (all reference standards) were obtained from the United States Pharmacopeia (São Paulo, SP, Brazil).

CP-coated paper characterization

Initially, PPy, PAni and [Poly(Py-*co*-Ani)] were characterized to evaluate the paper's surface, composition, morphology and thermal stability using attenuated total reflectance Fourier transform infrared (ATR-FTIR) spectroscopy, thermogravimetry analysis (TGA), atomic force microscopy (AFM) and scanning electron microscopy coupled to energy dispersive X-ray spectroscopy (SEM/EDS).

The ATR-FTIR analyses were performed in a Spectrum 400 MID/NIR FTIR (Perkin Elmer®, Waltham, MA, USA) with an ATR accessory (Zinc Selenide crystal) for data acquisition. ATR-FTIR spectra were acquired in a single mode in the region ranging from 4000 to 650 cm^{-1} with a resolution of 4 cm^{-1} by averaging 32 scans for each sample.

Thermogravimetry analyses were performed using the CP in powder form. The equipment employed was a DTG-60H model simultaneous analysis (Shimadzu®, Kyoto, Japan), varying from ambient temperature 23±2°C to 1000°C at a heating rate of 2°C min^{-1} in the air at atmospheric pressure.

AFM analyses were performed using chromatographic paper (Whatman Grade 1, 11 μm pores, GE Healthcare, USA) before and after *in situ* polymerization with PPy, PAni, and Poly(Py-*co*-Ani). All experiments were performed using a confocal microscope Alpha 300R (WITec/Wissenschaftliche und Technologie GmbH® Instrumente, Ulm, Germany). Topographical images by AFM analyses were obtained in non-contact mode (regions selected by using the light microscope), with a Si_3N_4 cantilever, at a nominal constant of 42 Nm^{-1}, a resonance frequency of ≈ 285 kHz, a scan rate of 0.3-1.0 Hz and a scan size of 2,500-10,000 nm. The peak-to-peak height parameter was used to evaluate the surface morphology roughness. The topographic images, phase images, and light microscopy images were collected simultaneously. Variations in the phase images can be used to estimate physical-chemical properties such as surface hardness, adherence, and viscoelasticity. In addition to topography,

histogram graphics were assembled using the WITec software for better characterization of the images.

For SEM analyses, the 500 SSX Shimadzu® (Kyoto, Japan) equipment was used, and the CP-coated papers were bonded with carbon glue in an electrically conductive support and coated with a 20 nm layer of gold (Super Cool Sputtering System Bal-Tec® SCD 050, Germany) to improve image quality.

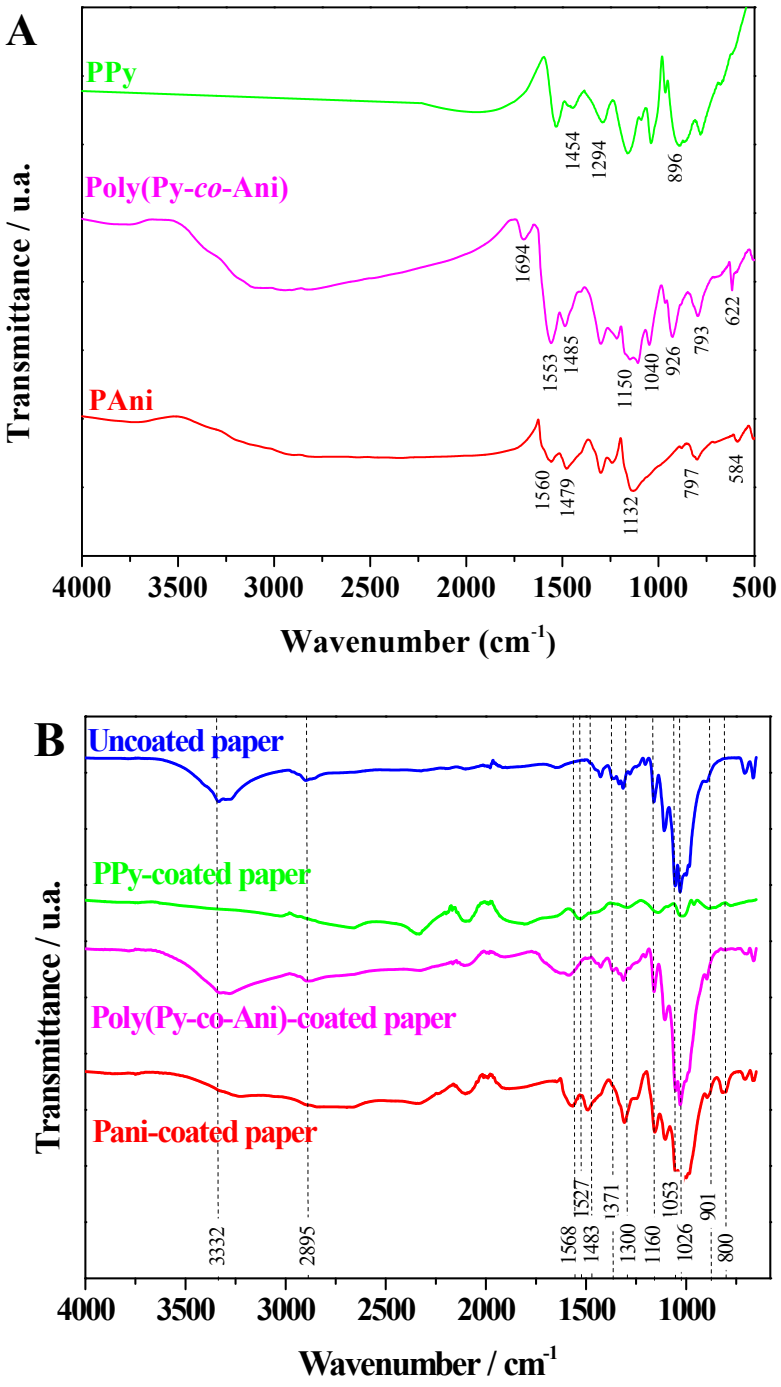

Fig. S1. FTIR spectra of conductive polymers as (A) powder, (B) uncoated and coated papers (chromatographic paper, Whatman, 20 µm pores, GE Healthcare, USA).

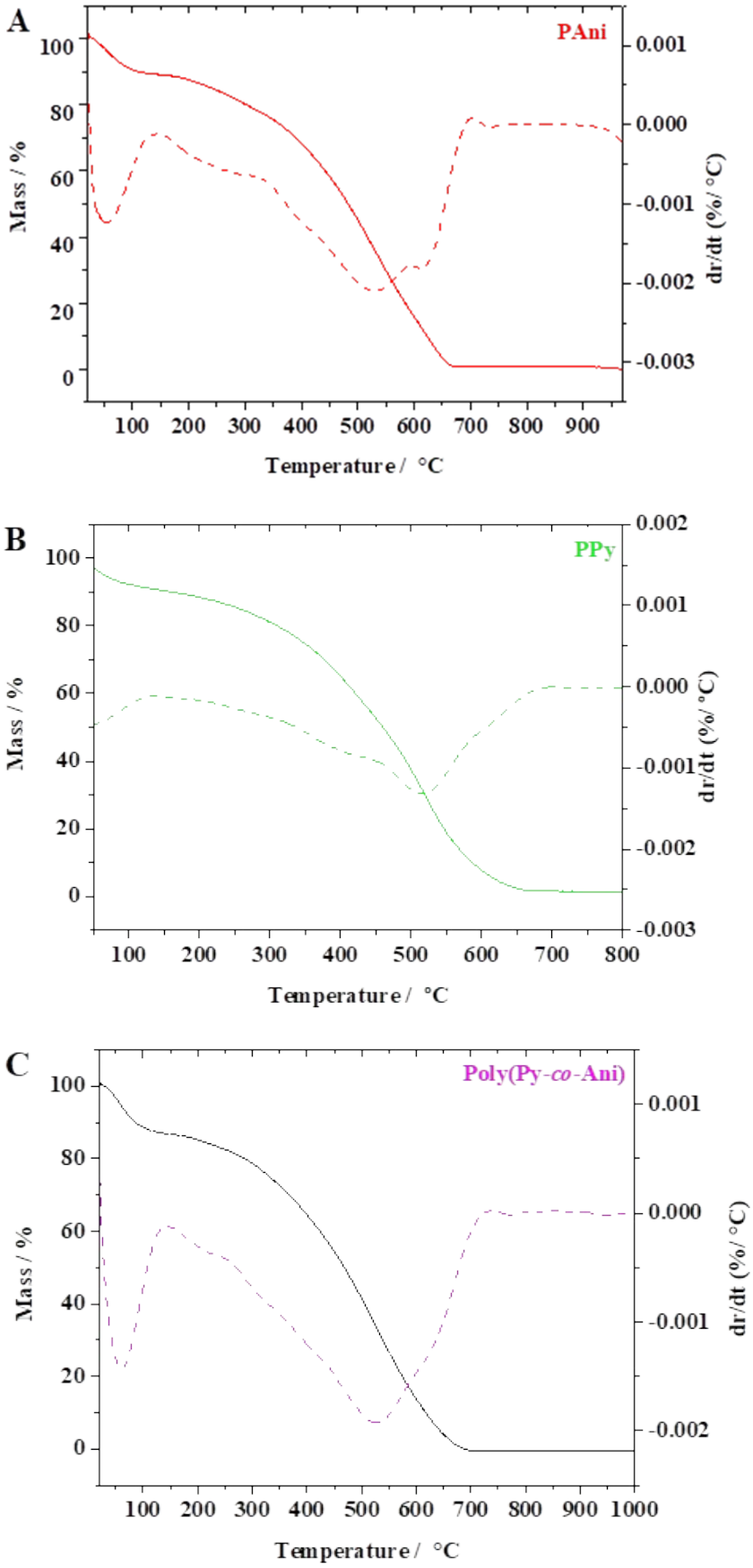

Fig. S2. TGA curves of (A) PAni, (B) PPy, and (C) Poly(Py-*co*-Ani).

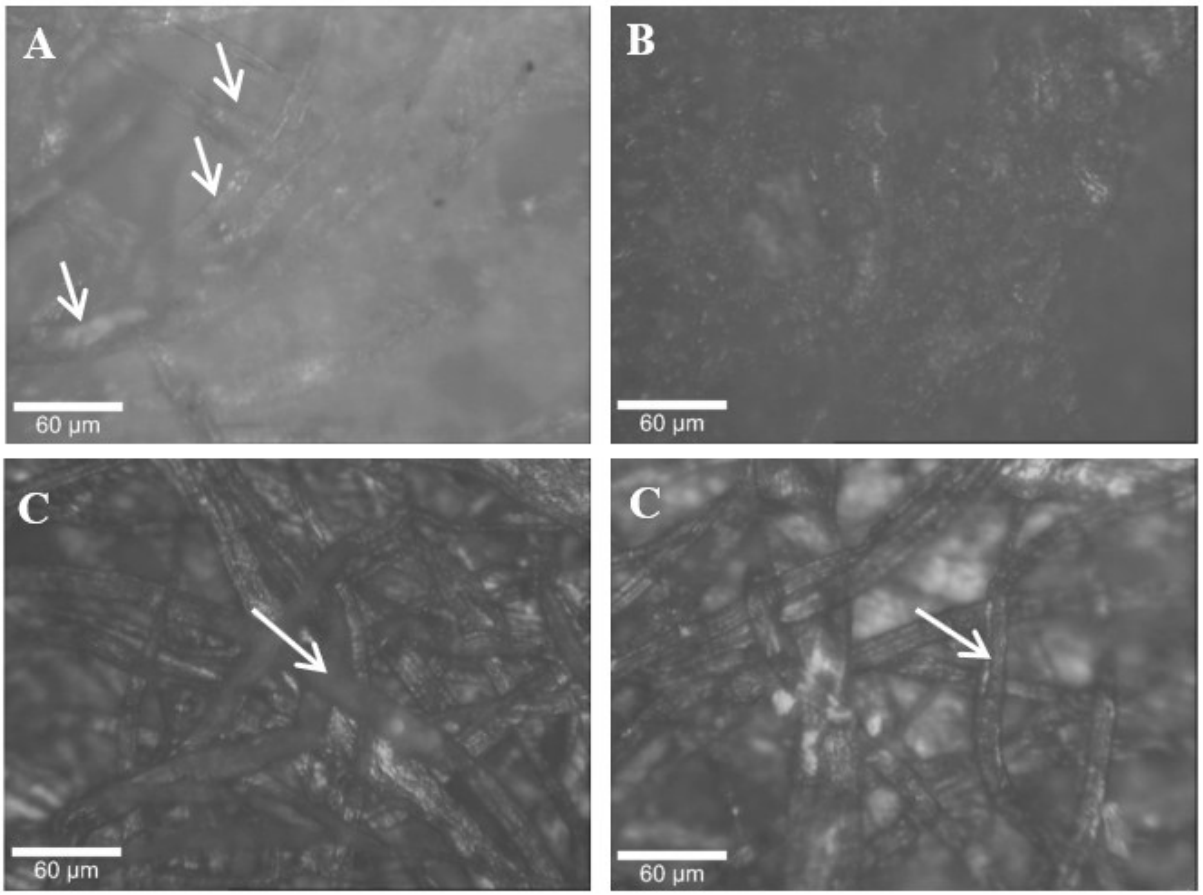

Fig. S3. LM images of **(A)** Whatman chromatographic paper showing the cellulose fibers (arrows) profile; **(B)** and the paper after *in situ* polymerization using PPy, in which fibers are not evident; and using **(C)** Poly(Py-*co*-Ani)-coated paper, in which the fiber structures are kept intact; and using (**D)** PAni, wherein fibers are visible.

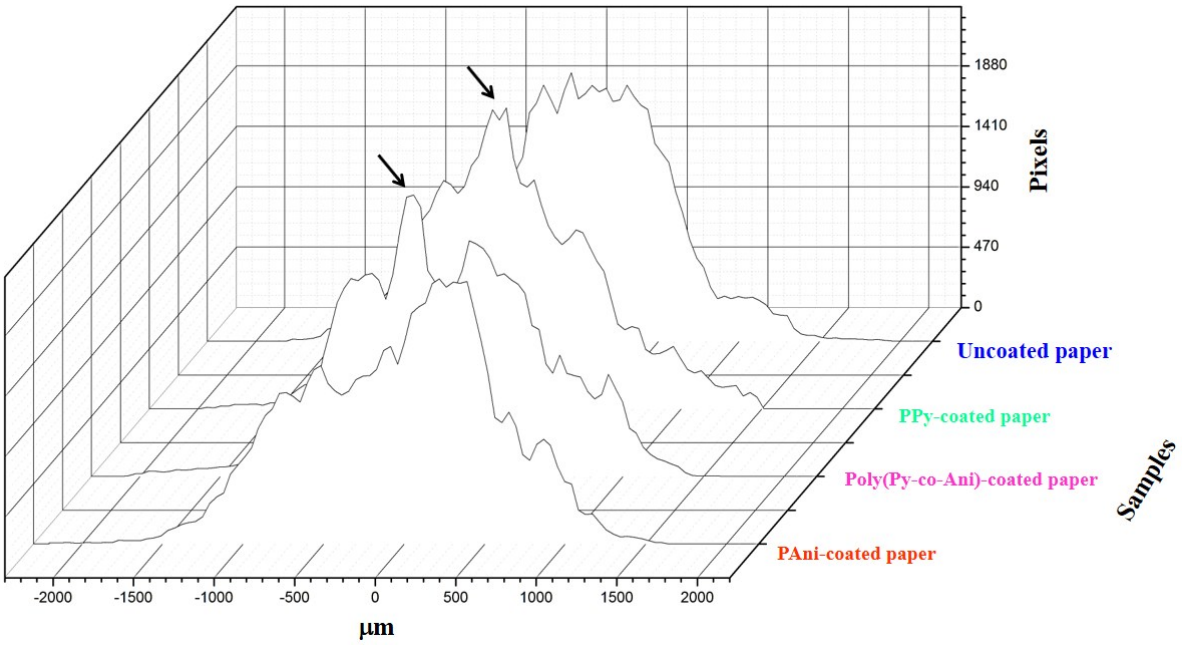

Fig. S4. Corresponding histograms of AFM topographic images of uncoated paper, PPy-coated paper, Poly(Py-*co*-Ani)-coated paper and PAni-coated paper.

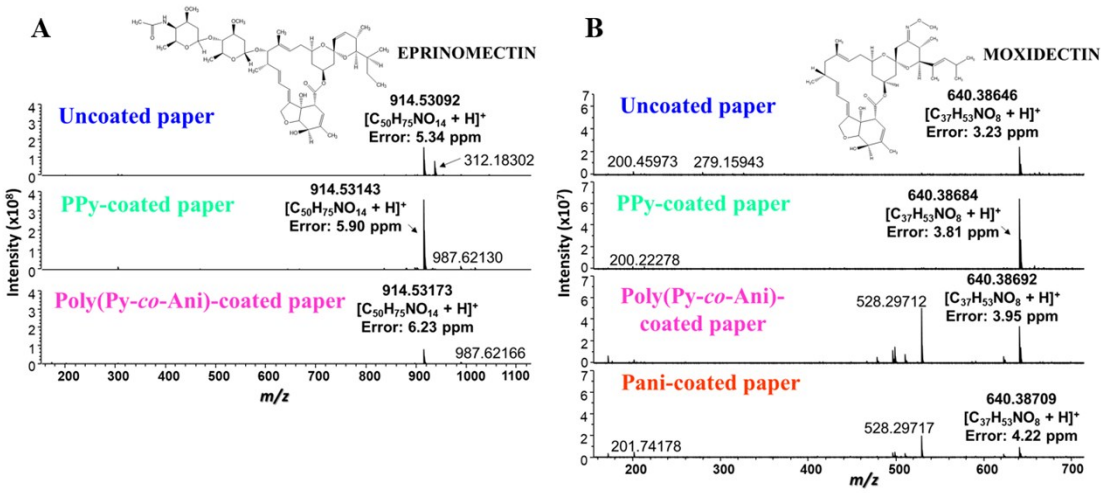

Fig. S5. PS(+)-FT-ICR mass spectra for analyses of (A) eprinomectin and (B) moxidectin using uncoated paper (Chromatographic paper), PPy-coated paper, Poly(Py-*co*-Ani)-coated paper, and PAni-coated paper.

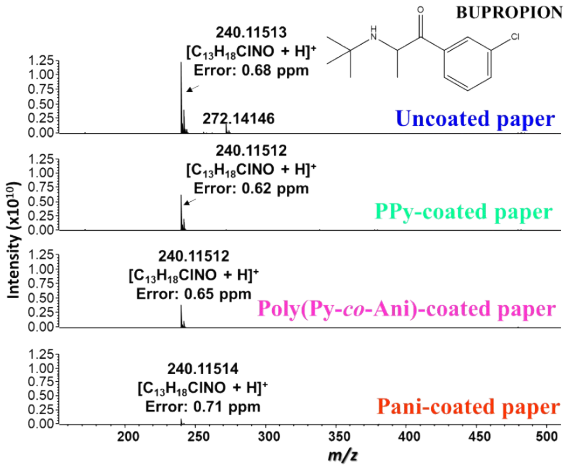

Fig. S6. PS(+)-FT-ICR mass spectra for analyses of bupropion using uncoated paper (Chromatographic paper), PPy-coated paper, Poly(Py-*co*-Ani)-coated paper, and PAni-coated paper.

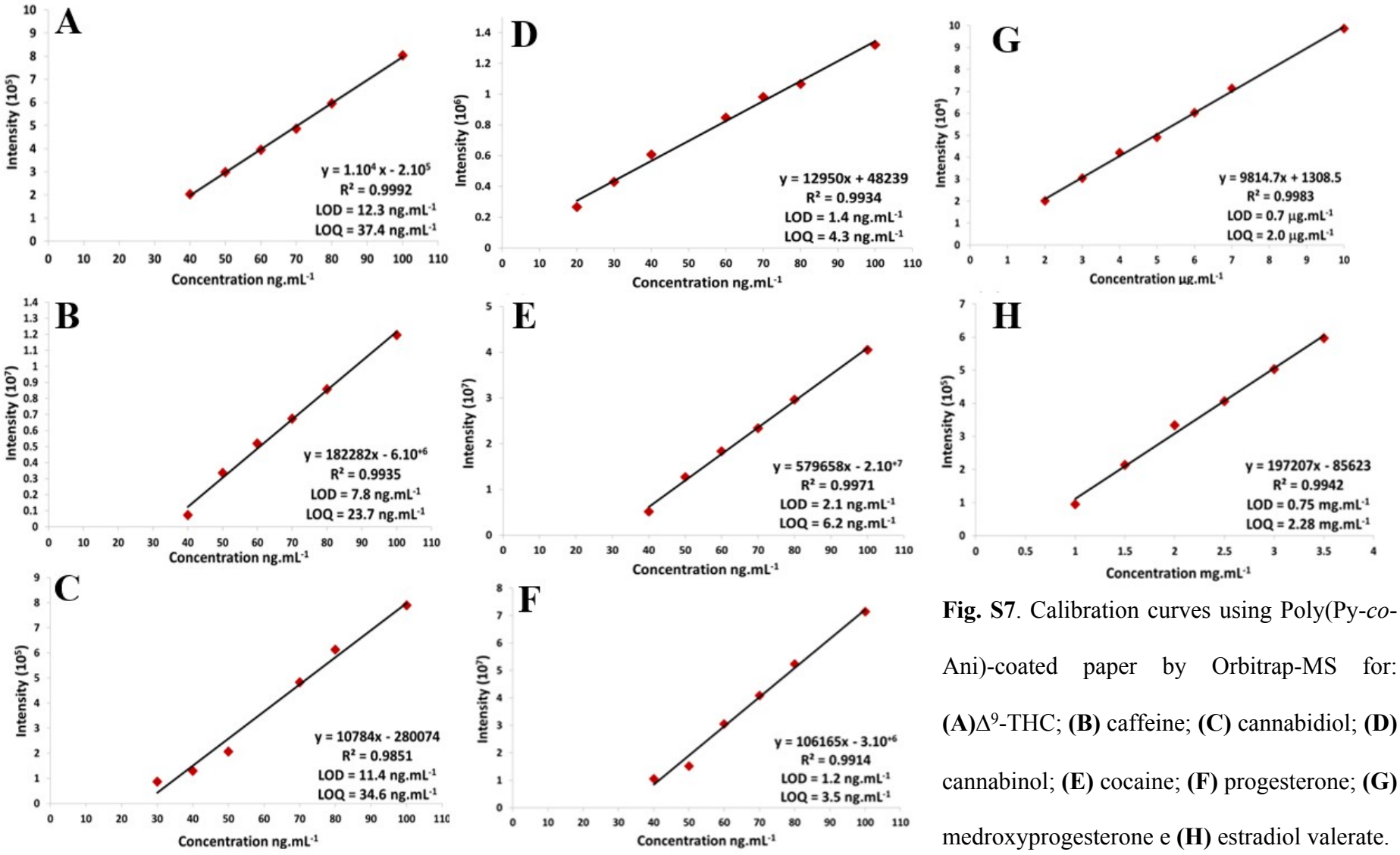

Fig. S7. Calibration curves using Poly(Py-*co*-Ani)-coated paper by Orbitrap-MS for: **(A)**Δ^9-THC; **(B)** caffeine; **(C)** cannabidiol; **(D)** cannabinol; **(E)** cocaine; **(F)** progesterone; **(G)** medroxyprogesterone e **(H)** estradiol valerate.

Table S1. PS(+)-FT-ICR data for avermectins and bupropion and its metabolites.

		Intensity	*m/z* measured	Error (ppm)	Res.[a]	DBE[b]	*m/z* standard
abamectin	Whatman	7.0×10^7	890.53056	5.09	22693	12	$[C_{48}H_{72}O_{14} + NH_4]^+$ 890.52603
	PPy	7.3×10^7	890.53111	5.70	22686		
	PPy/PAni[c]	5.6×10^7	890.53134	5.96	22907		
	PAni	-	-	-	-		
doramectin	Whatman	7.6×10^7	916.54654	5.30	22015	13	$[C_{50}H_{74}O_{14} + NH_4]^+$ 916.54168
	PPy	5.7×10^7	916.54683	5.61	22219		
	PPy/Ani[c]	-	-	-	-		
	PAni	-	-	-	-		
eprinomectin	Whatman	1.6×10^8	914.53092	5.34	22019	14	$[C_{50}H_{75}NO_{14} + H]^+$ 914.52603
	PPy	3.6×10^8	914.53143	5.90	22052		
	PPy/PAni[c]	7.8×10^7	914.53173	6.23	22073		
	PAni	-	-	-	-		
ivermectin	Whatman	3.3×10^7	892.54644	5.33	22741	12	$[C_{48}H_{74}O_{14} + NH_4]^+$ 892.54756
	PPy	9.2×10^6	892.54681	5.75	23868		
	PPy/PAni[c]	2.4×10^7	892.54699	5.94	24687		
	PAni	-	-	-	-		
moxidectin	Whatman	2.4×10^7	640.38646	3.23	31495	12	$[C_{37}H_{53}NO_8 + H]^+$ 640.38439
	PPy	6.4×10^7	640.38684	3.81	31544		
	PPy/PAni[c]	3.4×10^7	640.38692	3.95	31710		
	PAni	9.2×10^6	640.38709	4.22	31554		
bupropion	Whatman	1.2×10^{10}	240.11513	0.68	82907	5	$[C_{13}H_{18}ClNO + H]^+$ 240.11497
	PPy	6.3×10^9	240.11512	0.62	83254		
	PPy/PAni[c]	3.9×10^9	240.11512	0.65	83135		
	PAni	1.0×10^9	240.11514	0.71	83199		
erythrohydro bupropion	Whatman	1.1×10^{10}	242.13083	0.87	82713	4	$[C_{13}H_{20}ClNO + H]^+$ 242.13062
	PPy	7.2×10^7	242.13080	0.74	82762		
	PPy/PAni[c]	1.5×10^8	242.13080	0.73	82900		
	PAni	1.0×10^8	242.13076	0.60	82353		
hidroxybupropion	Whatman	8.7×10^7	256.11004	0.59	78311	5	$[C_{13}H_{18}ClNO_2 + H]^+$ 256.10988
	PPy	1.9×10^9	256.11005	0.67	78446		
	PPy/PAni[c]	3.1×10^8	256.11001	0.49	76604		
	PAni	3.1×10^8	256.11008	0.78	78278		
Threohydro bupropion	Whatman	2.0×10^{10}	242.13083	0.86	82415	4	$[C_{13}H_{20}ClNO + H]^+$ 242.13062
	PPy	4.4×10^9	242.13080	0.73	82254		
	PPy/PAni[c]	3.9×10^9	242.13079	0.71	82322		
	PAni	9.2×10^8	242.13080	0.76	82519		

[a] Resolving Power; [b] Double Bond Equivalent; [c] Poly(Py-*co*-Ani).